Mechanical response of bilayer graphene under different loading modes

Euclides Mesquita[1], Daniela A. Damasceno[2],Otávio A. Tovo[1]

[1]*School of Mechanical Engineering, University of Campinas*
R. Mendeleyev, 200, Cidade Universitária, Campinas, 13083-860, SP, Brazil
euclides@fem.unicamp.br, otaviotovo@hotmail.com
[2]*Institute of Physics, University of São Paulo*
Rua do Matão 1371, São Paulo, 05508-090, SP, Brazil
daniela.damasceno@usp.br

Abstract. Carbon-based materials remain promising nanostructures for the development of efficient and innovative nanotechnologies due to their outstanding properties. Among these nanostructures, bilayer nanoporous graphene has been considered a good candidate for applications involving water desalination, energy storage, among others. However, the remarkable mechanical properties of the pristine graphene sheets are strongly affected by the presence of nanoporous. Thus, in this study, molecular dynamics (MD) were conducted to investigate bilayer nanoporous graphene's mechanical response under several loading and constraints. Our results reveal that the introduction of porosity in the graphene's layers decrease significantly their fracture strain. The idea of adding a second, constrained layer or constrained patches of different sizes, to improve the mechanical tensile properties of the upper layer yielded no significant modification of its mechanical properties. This behavior suggests that to influence the mechanical properties of a defect or porous graphene layer by adding parallel layers or repair patches, other kinds of bonds, not van der Waals, must be created among the layers.

Keywords: bilayer graphene, nanoporous, mechanical properties, molecular simulations.

1 Introduction

Carbon-based materials, such as graphene [1], remain an excellent promise for the development of efficient and innovative nanotechnologies due to their outstanding mechanical and electronic properties [2,3]. Nowadays, there is increasing interest in developing nanofluidic systems, molecular sieves, among others [4–6]. Bilayer nanoporous graphene has been considered a good candidate for such applications [7]. However, the remarkable mechanical properties of the pristine graphene sheets are strongly affected by the presence of nanoporous [8]. Therefore, a fundamental understanding of the mechanical response of bilayer nanoporous graphene under different loading and constraint is crucial for future applications.

Several studies have been conducted to study the mechanical properties of carbon-based materials [9]. For instance, previous studies investigated the effects of chirality [8], temperature [10], topological defects [8,11], nanoporous [12], and boundary conditions [13] on the mechanical properties of monolayer graphene. Other studies investigated the same effects considering the carbon nanotubes [14–16] and nanoribbons [17–19], in which both nanotubes and nanoribbons are obtained from graphene sheets. Several other studies [20,21] performed molecular simulations and first-principles calculations to study the mechanical properties of bilayer and multilayer graphene. Although there are many studies regarding the mechanical properties of graphene, little is known about the bilayer nanoporous graphene.

In this study, molecular simulations (MD) were conducted to investigate the bilayer nanoporous graphene's mechanical response. Different loading and constraints were considered to investigate the tensile properties dependence in respect to these boundary conditions. Initially, we considered pristine mono and bilayer

graphene. Later, the same study was performed for a bilayer nanoporous graphene considering different sizes for the first layer.

2 Method and model

MD simulations were carried out based on the adaptive intermolecular reactive bond order (AIREBO) [22] potential, using the LAMMPS (Large-scale Atomic/Molecular Massively Parallel Simulator) [23] package to investigate the mechanical response of bilayer nanoporous graphene. AIREBO is one of the most appropriate potential to simulate hydrocarbon systems since it considers both covalent and non-bonded interactions. This potential is formed by the reactive empirical bond order (REBO) potential (E_{ab}^{REBO}), Lennard Jones (LJ) (E_{ab}^{LJ}), and the torsional interactions (E_{cabd}^{tors}), as shown in eq. (1):

$$E^{AIREBO} = \frac{1}{2}\sum_a \sum_{b\neq a}\left[E_{ab}^{REBO} + E_{ab}^{LJ} + \sum_{c\neq a,b}\sum_{d\neq a,b,c} E_{cabd}^{tors}\right] \quad (1)$$

where the indices a, b, c, and d refer to individual atoms. The AIREBO cut-off radii was set as 2.0 Å, based on the previous studies [24]. Periodic boundary conditions were considered in all directions and a timestep of 0.5 fs was considered in all simulations. Initially, it was conducted an energy equilibration followed by a pressure equilibration at zero pressure through an isothermal-isobaric (NPT) ensemble. Then, the uniaxial tensile strain was performed along the zigzag direction by applying strain at a rate of 0.001 ps-1 in the x-direction. All MD simulations were carried out at a temperature of 10 K with the temperature controlled by the Nose-Hoover thermostat. A graphene sheet with 1500 atoms with dimensions of approximately 61 Å × 63 Å, Figs. 1(a) and (b), was used as the base model to create bilayer graphene, Fig. 1(c), and bilayer nanoporous graphene (See Figs. 3 and 4). The interlayer distance was considered 3.4 Å.

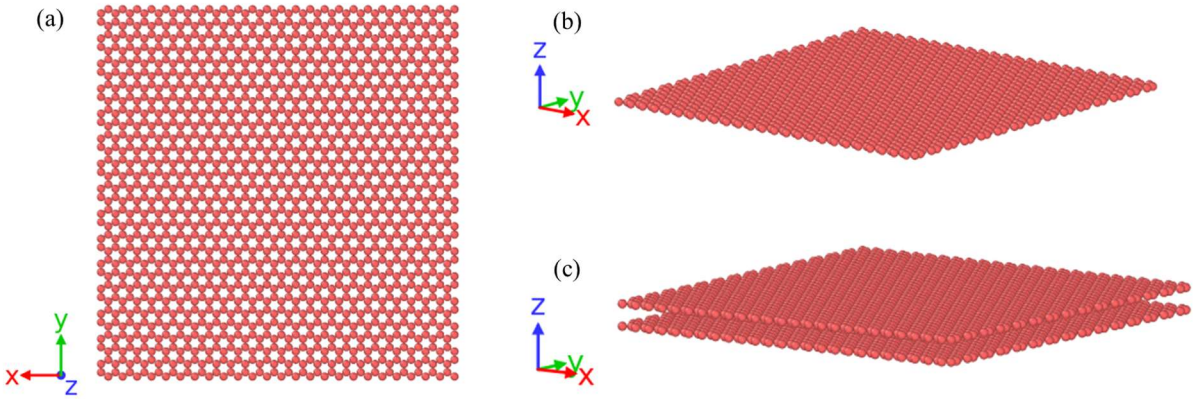

Figure 1. (a) and (b) pristine monolayer graphene, and (c) bilayer graphene.

3 Results and discussion

3.1 Mechanical response of bilayer graphene

In Fig. 2(d), we present the stress-strain curves for all three cases shown in Figs. 2(a)-(c) under uniaxial tensile strain along the x-direction (zigzag direction). No significant difference is observed in the mechanical response of the mono and bilayer graphene. These results are in agreement with those reported in [21]. For both cases (a) and (b), the fracture stress and strain are 111 GPa and 0.265, respectively. These results are in good agreement with the ones reported in the literature for the monolayer graphene, ranging from 98–138 GPa and 0.12 to 0.28 in the zigzag direction [11,13]. For case (c), in which the lower graphene layer is constrained and the upper one a tensile strain is imposed, there is only a small variation regarding the levels of strain fracture. In fact, the introduction of a fixed second constrained graphene layer resulted in a slightly smaller fracture strain for the first layer.

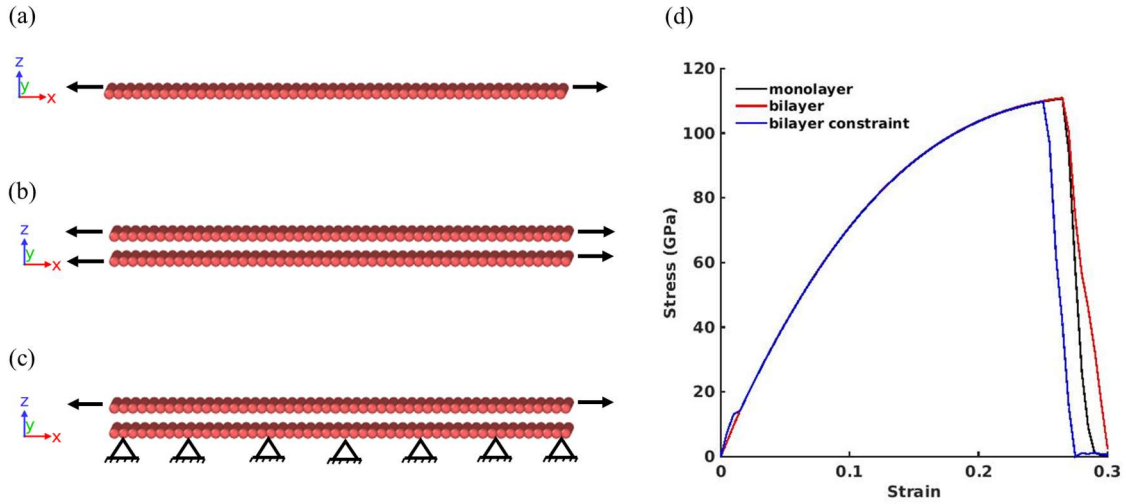

Figure 2. Mechanical response of pristine (a) monolayer graphene, (b) bilayer graphene, and (c) bilayer graphene with constraints, and (d) stress-strain curves of the systems shown in (a), (b), and (c).

3.2 Mechanical response of bilayer nanoporous graphene

In the second numerical example, the stress-strain properties of mono- and bilayer nanoporous graphene is addressed. Figures 3(a) and 3(b) show the meshes with vacancy or porosity.

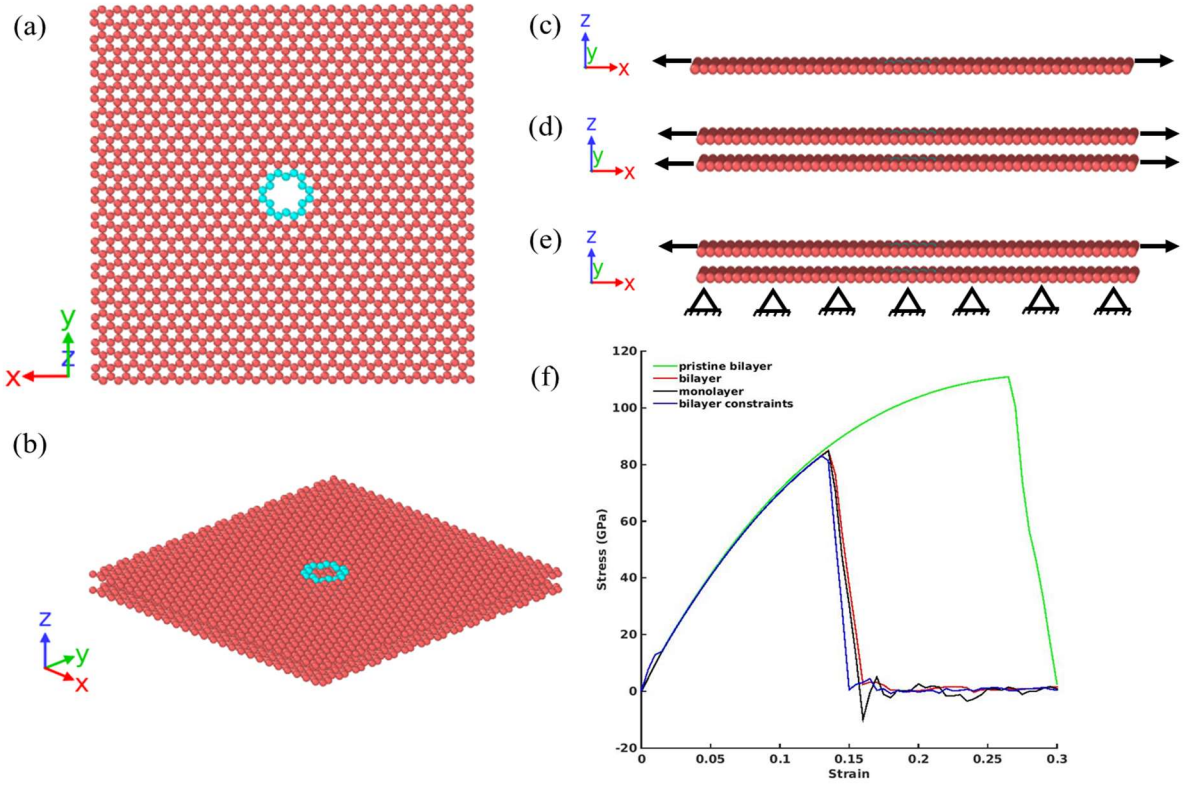

Figure 3. (a) monolayer nanoporous graphene, (b) bilayer nanoporous graphene, (c) boundary conditions applied on the system (a), (d) boundary conditions applied on the system (b), (e) boundary conditions applied on the system (b), (d) stress-strain curves of the pristine bilayer graphene (green curve), monolayer nanoporous graphene (black curve), bilayer nanoporous graphene (red curve), and bilayer nanoporous graphene with the constraints in (e) (blue curve).

Figures 3(c)-(e) show the analyzed cases. A porous monolayer Fig. 3(c) and a porous bilayer Fig. 3(d) are strained in the zigzag directions. For the case illustrated in figure 3(e), the degrees of freedom (atoms) of the lower layer are restricted and the upper layer is strained. Results are shown in Fig. 3(f), where the stress-strain curves for a pristine bilayer are also shown (green curve). The first striking point of these results is that the introduction of the nanoporous in the graphene sheets causes a significant reduction of the fracture strain on the specimen. The results for the porous monolayer (black curve) and the bilayer (red curve) are almost indistinguishable from each other. This result is consistent with the analysis performed in the previous session (3.1). For the case of the strained upper layer and a constrained lower layer, the results are given in the blue curve. Again, the constrained degrees of freedom of the lower layer have no influence on the stress-strain behavior of the upper nanoporous layer.

3.3 Mechanical response of monolayer nanoporous graphene with repair patch

In this section, we investigated the mechanical response of a monolayer nanoporous graphene with repair patches of different sizes. The first case (called 1) is shown in Fig. 4(c). Here the repair presents the same size as the nanoporous graphene layer. In the second case (called 2), the repair is smaller compared to case 1, as shown in Fig. 4(d), and the repair on case 3 is smaller compared to case 2, as shown in Fig. 4(e). For the three cases, the repair layer is fully constrained.

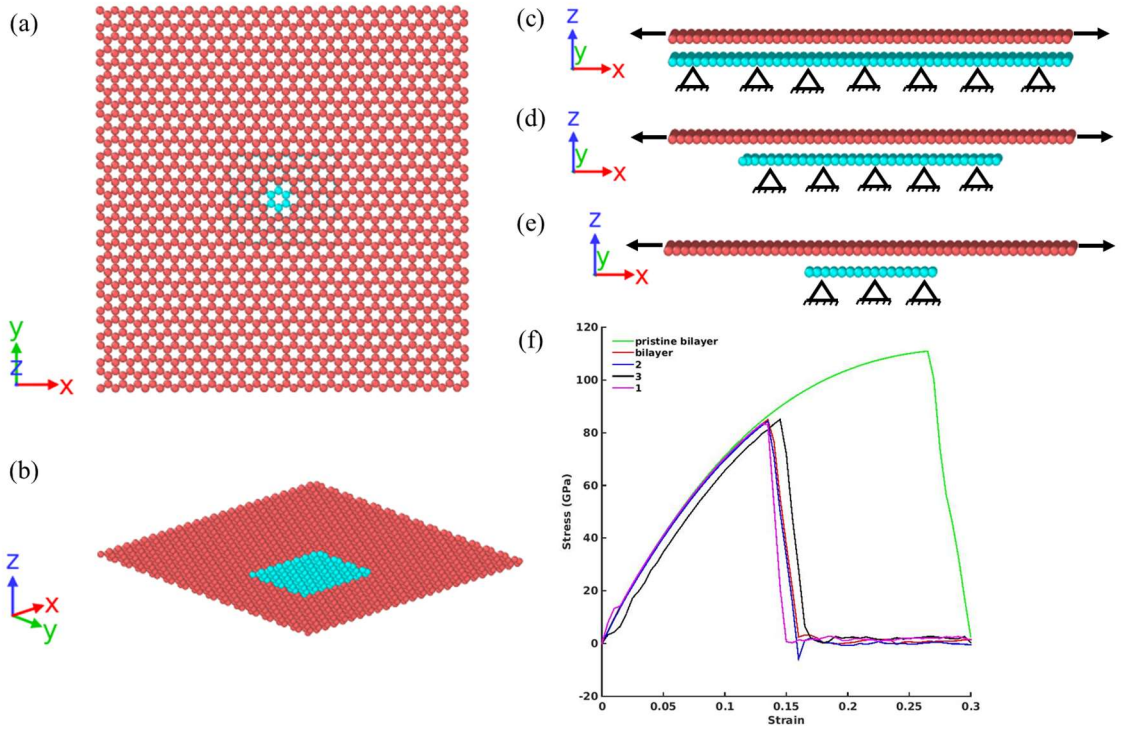

Figure 4. (a) and (b) Sample of a monolayer nanoporous graphene with a repair, (c) case 1: boundary conditions applied on the monolayer nanoporous graphene with a large repair, (d) case 2: boundary conditions applied on the monolayer nanoporous graphene with a smaller repair, (e) case 3: boundary conditions applied on the monolayer nanoporous graphene with the smaller repair, and (f) stress-strain curves of the system shown in (c) (purple curve), (d) (blue curve), (e) (black curve), bilayer nanoporous graphene (red curve), and pristine bilayer (green curve).

An analysis of the results presented in Fig. 4 shows that the size of the repair patches does not influence the mechanical stress-strain properties of the nanoporous upper layer.

4 Conclusions

The simulations conducted on the mechanical stress-strain properties of the pristine and porous, mono- and bilayer graphene arrangements suggest that the presence of the second, passive layer, does not influence the behavior of the upper, strained, layer. The introduction of a vacancy or a porosity in the layers decreases significantly the fracture strain of the specimen. The idea of adding a second, constrained layer or constrained patches of different sizes, to improve the mechanical tensile properties of the upper layer yielded no significant modification of its mechanical properties.

There is a plausible explanation for this behavior. The chemical bonds within the graphene layer are of the covalent type. These bonds yield an in-plane elasticity modulus for the pristine layer of approximately 1TPa (E=1TPa) according to the literature [21]. On the other hand, the interaction between the graphene layers is controlled by van der Waals bonds. The in-plane shear modulus for two pristine graphene layers has been reported to vary between 480 GPa to 600 GPa according to the loading direction (zigzag or armchair) [21]. So, the van der Waal bonds between the layers yield elasticity moduli that are 3 orders of magnitude smaller than the one generated by in-plane covalent bonds. The interaction of a second layer or patches of distinct sizes, based on van der Waals interactions, cannot restore or improve the original mechanical properties of the pristine graphene layer, in which a vacancy or a nanoporous has been introduced. This suggests that to influence the mechanical properties of a defect or porous graphene layer by adding parallel layers or repair patches, other kinds of bonds, not van der Waals, must be created among the layers.

Acknowledgements. The research leading to this work was funded by the São Paulo Research Foundation (Fapesp) grant FAPESP CEPID Process 2013/08293-7 and Coordenação de Aperfeiçoamento de Pessoal de Nível Superior - Brasil (CAPES) - Finance Code 001. DAD also thanks to the Research Centre for Gas Innovation, SHELL Brazil, and the financial support of FAPESP, grant 2020/01558-9.

Authorship statement. The authors hereby confirm that they are the sole liable persons responsible for the authorship of this work, and that all material that has been herein included as part of the present paper is either the property (and authorship) of the authors, or has the permission of the owners to be included here.

References

[1] K.S. Novoselov, A.K. Geim, S. V. Morozov, D. Jiang, Y. Zhang, S. V. Dubonos, I. V. Grigorieva, A.A. Firsov, Electric field in atomically thin carbon films, Science (80-.). 306 (2004) 666–669. https://doi.org/10.1126/science.1102896.

[2] C. Lee, X. Wei, J.W. Kysar, J. Hone, Measurement of the Elastic Properties and Intrinsic Strength of Monolayer Graphene, Science (80-.). 321 (2008) 385–388. https://doi.org/10.1126/science.1157996.

[3] M. Terrones, A.R. Botello-Méndez, J. Campos-Delgado, F. López-Urías, Y.I. Vega-Cantú, F.J. Rodríguez-Macías, A.L. Elías, E. Muñoz-Sandoval, A.G. Cano-Márquez, J.C. Charlier, H. Terrones, Graphene and graphite nanoribbons: Morphology, properties, synthesis, defects and applications, Nano Today. 5 (2010) 351–372. https://doi.org/10.1016/j.nantod.2010.06.010.

[4] W. Yuan, J. Chen, G. Shi, Nanoporous graphene materials, Mater. Today. 17 (2014) 77–85. https://doi.org/10.1016/j.mattod.2014.01.021.

[5] D. Cohen-Tanugi, J.C. Grossman, Water desalination across nanoporous graphene, Nano Lett. 12 (2012) 3602–3608. https://doi.org/10.1021/nl3012853.

[6] H. Liu, Z. Chen, S. Dai, D.E. Jiang, Selectivity trend of gas separation through nanoporous graphene, J. Solid State Chem. 224 (2015) 2–6. https://doi.org/10.1016/j.jssc.2014.01.030.

[7] K. Celebi, J. Buchheim, R.M. Wyss, A. Droudian, P. Gasser, I. Shorubalko, J. Il Kye, C. Lee, H.G. Park, Ultimate permeation across atomically thin porous graphene, Science (80-.). 344 (2014) 289–292. https://doi.org/10.1126/science.1249097.

[8] D.A. Damasceno, R.K.N.D. Rajapakse, E. Mesquita, R. Pavanello, Atomistic simulation of tensile strength properties of graphene with complex vacancy and topological defects, Acta Mech. (2020). https://doi.org/10.1007/s00707-020-02715-6.

[9] B. Cox, T. Hilder, J. Hill, N. Thamwattana, Modelling and Mechanics of Carbon based Nanostructured Materials, William Andrew: Oxford, UK, 2017.

[10] M.A.N. Dewapriya, R.K.N.D. Rajapakse, A.S. Phani, Atomistic and continuum modelling of temperature-dependent fracture of graphene, Int. J. Fract. 187 (2014) 199–212. https://doi.org/10.1007/s10704-014-9931-y.

[11] G. Rajasekaran, P. Narayanan, A. Parashar, Effect of point and line defects on mechanical and thermal properties of graphene: A review, Crit. Rev. Solid State Mater. Sci. 41 (2016) 47–71.

https://doi.org/10.1080/10408436.2015.1068160.
[12] Y. Liu, X. Chen, Mechanical properties of nanoporous graphene membrane, J. Appl. Phys. 115 (2014). https://doi.org/10.1063/1.4862312.
[13] G. Cao, Atomistic studies of mechanical properties of graphene, Polymers (Basel). 6 (2014) 2404–2432. https://doi.org/10.3390/polym6092404.
[14] H. Yazdani, K. Hatami, M. Eftekhari, Mechanical properties of single-walled carbon nanotubes: a comprehensive molecular dynamics study, Mater. Res. Express. 4 (2017) 055015. https://doi.org/10.1088/2053-1591/aa7003.
[15] M. Sammalkorpi, A. Krasheninnikov, A. Kuronen, K. Nordlund, K. Kaski, Mechanical properties of carbon nanotubes with vacancies and related defects, Phys. Rev. B. 70 (2004) 245416. https://doi.org/10.1103/PhysRevB.70.245416.
[16] H. Mori, Y. Hirai, S. Ogata, S. Akita, Y. Nakayama, Chirality Dependence of Mechanical Properties of Single-Walled Carbon Nanotubes under Axial Tensile Strain, Jpn. J. Appl. Phys. 44 (2005) L1307–L1309. https://doi.org/10.1143/JJAP.44.L1307.
[17] and N.R.A. H. Zhao, K. Min, Size and Chirality Dependent Elastic Properties of Graphene Nanoribbons under Uniaxial Tension, Nano Lett. (2013) 1–6. https://doi.org/10.1021/nl901448z.
[18] D.A. Damasceno, E. Mesquita, R.K.N.D. Rajapakse, R. Pavanello, Atomic-scale finite element modelling of mechanical behaviour of graphene nanoribbons, Int. J. Mech. Mater. Des. (2018) 1–13. https://doi.org/10.1007/s10999-018-9403-z.
[19] Y. Chu, T. Ragab, C. Basaran, The size effect in mechanical properties of finite-sized graphene nanoribbon, Comput. Mater. Sci. 81 (2014) 269–274. https://doi.org/10.1016/j.commatsci.2013.08.016.
[20] Q. Cao, X. Geng, H. Wang, P. Wang, A. Liu, Y. Lan, Q. Peng, A review of current development of graphene mechanics, Crystals. 8 (2018). https://doi.org/10.3390/cryst8090357.
[21] S.A. Hosseini Kordkheili, H. Moshrefzadeh-Sani, Mechanical properties of double-layered graphene sheets, Comput. Mater. Sci. 69 (2013) 335–343. https://doi.org/10.1016/j.commatsci.2012.11.027.
[22] S.J. Stuart, A.B. Tutein, J.A. Harrison, A reactive potential for hydrocarbons with intermolecular interactions, J. Chem. Phys. 112 (2000) 6472–6486. https://doi.org/10.1063/1.481208.
[23] S. Plimpton, Fast Parallel Algorithms for Short-Range Molecular Dynamics, J. Comput. Phys. 117 (1995) 1–19. https://doi.org/10.1006/jcph.1995.1039.
[24] A.R. Alian, S.A. Meguid, A critical study of the parameters governing molecular dynamics simulations of nanostructured materials, Comput. Mater. Sci. 153 (2018) 183–199. https://doi.org/10.1016/j.commatsci.2018.06.028.